Statistical thermodynamics of equilibrium polymers at interfaces

J. van der Gucht* and N. A. M. Besseling
Laboratory of Physical Chemistry and Colloid Science, Dutch Polymer Institute/Wageningen University, P.O. Box 8038, 6700 EK Wageningen, The Netherlands

(Received 11 October 2001; published 17 May 2002)

The behavior of a solution of equilibrium polymers (or living polymers) at an interface is studied, using a Bethe-Guggenheim lattice model for molecules with orientation dependent interactions. The density profile of polymers and the chain length distribution are calculated. For equilibrium polymers at a nonadsorbing surface it is found that the depletion layer thickness has a maximum. In dilute solutions it is proportional to the average radius of gyration of the polymers, which increases with increasing concentration. Above the overlap concentration it corresponds to the bulk correlation length, which decreases with increasing concentration. Furthermore, it is found that the surface region is predominantly occupied by the shorter chains. Both in dilute solutions and in a melt of equilibrium polymers, a very simple relation is found between the surface excess of a component and the chain length.

DOI: 10.1103/PhysRevE.65.051801 PACS number(s): 61.25.Hq, 05.50.+q, 05.70.Np, 36.20.−r

I. INTRODUCTION

Polymers have been the subject of great scientific interest. This has resulted in a broad spectrum of theoretical, numerical, and experimental techniques to investigate their properties, both in solution and at interfaces [1–3]. A special class of polymers are the so called equilibrium polymers, or living polymers. The difference from classical polymers is that the bonds in equilibrium polymers are reversible rather than covalent. As a result, the chain length distribution in such systems is not fixed, but is determined by thermodynamic equilibrium. Examples of equilibrium polymers are liquid sulfur [4–6], wormlike micelles [7], and supramolecular polymers based on hydrogen bonding [8].

The equilibrium between breakage and formation of bonds in equilibrium polymer solutions results in a polydisperse chain length distribution. This equilibrium distribution can be calculated using statistical mechanics. Within a mean-field approximation, originally by Flory, this yields an exponential chain length distribution [2,7,9]:

$$\phi(N) = N \frac{\phi_M}{\langle N \rangle^2} \exp\left(- \frac{N}{\langle N \rangle} \right), \tag{1}$$

where $\phi(N)$ is the volume fraction of chains of N segments, ϕ_M is the total volume fraction of monomers, and $\langle N \rangle$ is the number averaged chain length. The factor $\phi_M / \langle N \rangle^2$ normalizes the distribution, ensuring $\Sigma_N \phi(N) = \phi_M$. The average chain length is a function of the monomer concentration ϕ_M, the scission energy E that is needed to break a bond between two monomers, and the temperature T:

$$\langle N \rangle \simeq \phi_M^{1/2} \exp\left(\frac{E}{2kT} \right). \tag{2}$$

This result does not depend on the chain stiffness, so that it applies to flexible chains, semiflexible chains, and stiff rods. No direct measurements of the chain length distribution have been reported so far, due to experimental difficulties [7].

Because of their ''tunable'' properties, it may be advantageous to use equilibrium polymers rather than classical polymers in some applications, for example if special rheological properties are desired. In many practical systems, the behavior of the polymer molecules near surfaces is of great importance. An example is the use in colloidal systems, where polymers can enhance or diminish the colloidal stability [3,10–12]. Obviously, before equilibrium polymers can be used for such applications, it is necessary to understand their behavior near surfaces and their effect on the interactions between colloidal particles.

So far, only little attention has been paid to equilibrium polymers near surfaces. The interfacial behavior of classical polymers, on the other hand, is quite well understood [3]. The presence of a surface affects a polymer molecule in two ways: (i) it reduces the conformational entropy, and (ii) it may have an energetic interaction with the polymer segments. The equilibrium configuration is a result of the balance between these two factors. If there is a strong attraction between the surface and the polymer segments, the polymers are adsorbed. If, on the other hand, the adsorption energy is too small to compensate the entropy loss, the polymers are depleted from the surface. Both polymer adsorption and depletion can cause flocculation in colloidal systems [3,10–12].

Several theoretical models have been proposed to describe the behavior of monodisperse polymers at interfaces. Scheutjens and Fleer [3,13–16] developed a self-consistent-field lattice theory, based on a mean-field approximation, which proved to be successful in describing polymer adsorption and depletion. The concentration profile of polymer segments is calculated. For nonadsorbing polymers there is a region of lower polymer concentration next to the surface (the depletion layer). The thickness of this depleted region corresponds to the correlation length in the bulk of the polymer solution. Several regimes can be distinguished [3]. In dilute solutions the thickness of the depleted region is approximately equal to the radius of gyration R_g of the polymer

*Electronic address: jasper@fenk.wau.nl

coils. Within a mean-field approximation this radius of gyration scales with the chain length as $R_g \sim N^{1/2}$. Above the overlap concentration, the interactions between polymer coils become important. The coils interpenetrate and form a network. In good solvents, mean-field theory predicts a crossover to the so-called marginal regime, where binary interactions are dominant. This crossover occurs at a volume fraction $\phi^* \sim N^{-1}$. In the marginal regime the correlation length (which determines the depletion layer thickness) is independent of the chain length and decreases with increasing polymer concentration as $\xi_m \sim \phi^{-1/2}$. At higher polymer concentrations, a crossover to the concentrated regime is observed, where higher order interactions become important. The semidilute regime [1], which is important for flexible chains in a good solvent, cannot be described by the mean-field treatment. For a complete diagram of the different regimes in a polymer solution, see, for example, Refs. [3,17].

The theoretical description of polymer systems has focused mainly on monodisperse polymers. Equilibrium polymer solutions, however, are polydisperse. Furthermore, the chain length distribution is a function of the concentration [see Eqs. (1) and (2)]. A system of equilibrium polymers near a surface therefore adapts its chain length distribution in order to minimize the free energy. Since the entropic restrictions imposed by the surface are different for polymers of different chain lengths, the composition of the polymer solution close to the surface is expected to be different from the bulk composition. The entropy loss suffered by the longer chains is larger than that for the shorter chains, so that, in the absence of energetic interactions, the surface region is predominantly occupied by the shorter chains.

So far, only a few studies have dealt with polydisperse polymer systems near a surface. Hariharan *et al.* [18] used the Scheutjens-Fleer theory to study surface segregation in a bimodal polymer melt. Their results showed depletion of the long chains and net adsorption of the short chains, in agreement with what would be expected on the basis of entropic restrictions. Similar results were obtained by Hertanto and Dickman for semidilute solutions of polydisperse polymers using Monte Carlo simulations [19]. In a recent paper [20] we studied the effect of a surface on a polydisperse polymer melt with an arbitrary chain length distribution. A very simple relation was found between the surface excess of a component in the melt, its chain length, and its bulk concentration.

Schmitt *et al.* [21] presented an analytical model for a dilute solution of ideal equilibrium polymer chains confined between two repulsive walls. Excluded volume interactions were not accounted for in this approach. The depletion of equilibrium polymers from the gap resulted in an attractive force between the two plates, and a decrease of the average chain length in the gap. Milchev and Landau [22] did lattice Monte Carlo simulations on concentrated solutions of equilibrium polymers confined between two surfaces. Their results show that the surface region is preferentially occupied by short chains, which is in agreement with the results for polydisperse systems of unbreakable polymers [18,20]. Rouault and Milchev [23] used the same Monte Carlo algorithm to calculate the average chain length in a concentrated equilibrium polymer solution in a gap between two surfaces as a function of the gap size. Their results are in reasonable agreement with the analytical model of Schmitt *et al.* [21].

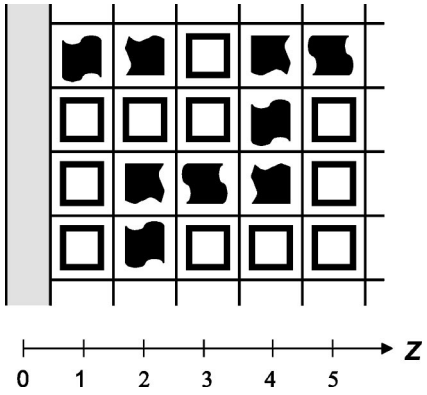

FIG. 1. A two-dimensional representation of a three-dimensional cubic lattice. Left of layer 1 there is an inert solid surface. Layers 1 to *M* contain solvent molecules (open squares) or bifunctional monomers (filled figures). The bonding groups of the monomers are denoted as curved faces.

In this paper we apply a lattice theory for molecules with orientation dependent interactions, developed by Besseling and Scheutjens [24], to a system of equilibrium polymers. The theory can be used in both homogeneous and inhomogeneous systems. In Besseling and Scheutjens's model correlations due to interactions between monomers are accounted for in a Bethe-Guggenheim approximation (also called the quasichemical approximation or first-order approximation). Besseling and co-workers successfully applied this theory to describe the structure of water and hydration forces [25–27].

In Sec. II we give a general description of the model. In Sec. III we present some results for equilibrium polymer solutions. In this paper we consider only flexible chains. First we consider a homogeneous solution and compare the present model to other mean-field models. Then we consider the case of nonadsorbing equilibrium polymers near a single surface, and compare these results to the depletion of unbreakable polymers. Finally, we look at the effect of a surface on the chain length distribution. In subsequent papers we will investigate chain stiffness, adsorption of equilibrium polymers, and the effect of equilibrium polymers on the surface forces.

II. THEORY

A. General description of the model

In this section, the general features of the theory are described. A method to calculate the chain length distribution is presented in Sec. II B. In Sec. II C we summarize the derivation of the partition function and the self-consistent-field equations for the equilibrium configuration. A more complete description of the theory can be found in Ref. [24].

A schematic representation of the model is depicted in Fig. 1. The volume that contains the equilibrium polymer solution is divided into a number of identical lattice sites. Each site contains either a solvent molecule or a bifunctional monomer. In order to deal with spatially inhomogeneous sys-

tems, the lattice is divided into M parallel lattice layers, numbered $z=1,2,\ldots,M$. Each layer is allowed to be occupied differently. The number of sites in each layer is denoted L. The surface area, and hence L, are taken infinitely large, so that edge effects can be ignored. By choosing the appropriate boundary conditions at $z=0$ and $z=M$, we can model a homogeneous solution, a solution adjoining a single solid surface, or a solution confined between two surfaces. The lattice coordination number q gives the number of neighboring sites that each lattice site has. In this paper we use a cubic lattice, in which $q=6$. Four of these neighboring sites are within the same lattice layer.

The surface of each molecule consists of q faces that are directed toward nearest neighbor sites. A bifunctional monomer has two different types of faces. Two of its q faces are the bonding groups, denoted as faces of type 2 (and in Fig. 1 represented as curved faces). The other $q-2$ faces of a monomer are denoted as faces of type 1. A monomer can have a number of different monomeric states. The state of a monomer is specified by the direction in which the two bonding groups are pointing. In the present paper we consider only completely flexible chains. Hence, there is no energy difference between linear states in which the two bonding groups are on opposite sides of the monomer and bent states where the two bonding groups make a 90° angle. Semiflexibility will be considered in a subsequent paper. The solvent molecules are isotropic, because all q faces of a solvent molecule are identical (these are denoted as faces of type 0). Solvent molecules therefore have no distinguishable states.

The number of molecules of type A having state σ that are located at layer z is denoted $n_A^\sigma(z)$. The subscript A denotes either a monomer (M) or a solvent (S) molecule. Every lattice site is occupied by either a monomer or a solvent molecule, so that the following constraint needs to be satisfied:

$$\sum_A n_A = n_M + n_S = ML, \tag{3}$$

where $n_A=\Sigma_{\sigma,z}n_A^\sigma(z)$ is the total number of molecules of type A in the system. The number of faces of type α ($=0$, 1, or 2) in layer z pointing in direction d is denoted $n_\alpha^d(z)$. Obviously, the distribution of faces is directly related to the distribution of molecule states. The number of contacts between faces of type α with direction d at sites in layer z and faces of type β is denoted $n_{\alpha\beta}^d(z)$. One of these contact types (2-2) denotes the formation of bonds between monomers. If the layer z and the direction d of a face α are specified, then the layer number and the direction of the face that makes contact with that face α are fixed. It is located at layer $z+\underline{d}$, by which we denote the layer at which d is directed from a site in layer z (here $\underline{d}$ can have the values -1, 0, or $+1$), and it has the opposite direction to d, denoted $-d$. Obviously, $n_{\alpha\beta}^d(z)=n_{\beta\alpha}^{-d}(z+\underline{d})$. For the distribution of contacts and faces the following relation should hold:

$$\sum_\beta n_{\alpha\beta}^d(z) = n_\alpha^d(z) \tag{4}$$

for all α, z, and d.

Site fractions of monomers, faces, and contacts are defined as $\phi_A^\sigma(z)\equiv n_A^\sigma(z)/L$, $\phi_\alpha^d(z)\equiv n_\alpha^d(z)/L$, and $\phi_{\alpha\beta}^d(z)\equiv n_{\alpha\beta}^d(z)/L$. They can be considered as probability distributions for sites to be occupied in a certain way.

A first-order or quasichemical approximation is used to calculate the occupation of the lattice sites. Correlations between neighboring sites are accounted for in this approach, but pairs of sites are occupied independently. This approach goes beyond the Bragg-Williams or random-mixing approximation, which assumes the occupation of individual sites to be stochastically independent. The contact probability $\phi_{\alpha\beta}^d(z)$ is related to the pair distribution function:

$$\psi_{\alpha\beta}^d(z)\equiv\frac{\phi_{\alpha\beta}^d(z)}{\phi_\beta^{-d}(z+\underline{d})}, \tag{5}$$

which is the conditional probability to find a face of type α, provided that it is located in layer z and points in direction d at a face of type β. In case the occupancy of nearest neighbor sites is stochastically independent, as in the Bragg-Williams approximation, $\psi_{\alpha\beta}^d(z)$ is independent of β. The contact probability for this case is simply given as the product of the occupation probabilities of each of the sites:

$$\phi_{\alpha\beta}^{d*}(z)=\phi_\alpha^d(z)\phi_\beta^{-d}(z+\underline{d}), \tag{6}$$

where the asterisk indicates a random distribution of contacts. Generally the distribution of contacts differs from the random distribution however, because low energy contacts (i.e., bonds between monomers) are favored over high energy contacts.

A bond between two neighbor monomers is formed if two of their bonding groups (type 2 faces) point toward each other. The strength of such a bond is determined by the contact energy $u_{22}=-E$ between two bonding groups. If E is large, 2-2 contacts will be favored and long chains will be formed. We take all contact energies $u_{\alpha\beta}$ between other combinations of faces (of monomers and solvent) equal to zero. This implies that we are dealing with a good solvent. All interaction energies with the surface are set to zero as well, so there is no preferential interaction of either monomers or solvent with the surface.

For a solution of equilibrium polymers in contact with a surface, the polymer concentration next to the surface will in general be different from the bulk concentration. The excess amount of monomers at the surface, expressed in equivalent lattice layers, is defined as

$$\theta_M^{\mathrm{ex}}=\sum_{z=1}^{M}[\phi_M(z)-\phi_M^b], \tag{7}$$

where ϕ_M^b is the bulk volume fraction of monomers. If depletion occurs, θ_M^{ex} is negative.

B. Chain length distribution

The formation of chains is a consequence of the formation of contacts between bonding groups (faces of type 2). The

chain length distribution can be calculated from the distribution of monomers and contacts over the lattice layers.

The volume fraction of monomers at layer z that have a chain fragment of $N-1$ monomers bound to one of its bonding groups and of which the *other* bonding group points in direction d is denoted as $\phi_M^d(z,N)$. Furthermore, the probability to find a monomer in layer z with a bonding group in direction d, with connected at *that* bonding group a chain fragment of $N-1$ other monomers, is denoted as $P^d(z,N)$.

Obviously,

$$P^d(z,1)=\phi_2^d(z)-\phi_{22}^d(z) \tag{8}$$

gives the probability to find an *end* segment at z with a nonbonded bonding group pointing in direction d.

For $N>1$,

$$P^d(z,N)=\phi_M^{-d}(z+\underline{d},N-1)\psi_{22}^d(z) \tag{9}$$

[this is quite analogous to Eq. (5)]. The first factor on the right hand side gives the probability of finding at layer $z+d$ the last segment of a fragment of $N-1$ segments, with the remaining bonding group pointing in direction $-d$, toward a site at z. The factor $\psi_{22}^d(z)$ gives the probability that this chain fragment is linked to another monomer at z.

Using Eqs. (8) and (9), all $\phi_M^d(z,N)$ can be obtained through the recurrence relation

$$\phi_M^d(z,N)=\sum_{d'} P^{d'}(z,N)P_2^{d|d'}(z). \tag{10}$$

The first factor under the summation gives the probability to find at layer z an Nth segment of a chain, with connected at direction d' a chain fragment of $N-1$ other monomers. The second factor $P_2^{d|d'}(z)$ gives the probability that one bonding group of a monomer at z has direction d, provided that the other has direction d'. This probability can be calculated if the distribution of monomer states $\{\phi_M^\sigma(z)\}$ is known, because the direction of the bonding groups is specified for each state. The product $P^{d'}(z,N)P_2^{d|d'}(z)$ yields the volume fraction of monomers at z that have a chain fragment of $N-1$ other monomers bound to a bonding group with direction d', and of which the other bonding group has direction d.

Equation (10) with Eq. (8) yields simply the volume fraction of chain ends at z:

$$\phi_M(z,1)=\sum_d \phi_M^d(z,1)=\sum_d [\phi_2^d(z)-\phi_{22}^d(z)] \tag{11}$$

from which the number weighted average chain length is obtained readily:

$$\langle N\rangle=\frac{\sum_z \phi_M(z)}{\frac{1}{2}\sum_z \phi_M(z,1)}. \tag{12}$$

The volume fraction of chains of N segments in the system can be calculated as

$$\phi(N)=\frac{N}{2M}\sum_{z,d}\phi_M^d(z,N)[1-\psi_{22}^{-d}(z+\underline{d})], \tag{13}$$

where the factor $\frac{1}{2}$ corrects for double counting of the chains. The factor in square brackets denotes the probability that a bonding group (of the Nth monomer) at layer z pointing in direction d is *not* linked to another monomer.

In general, the chain length distribution next to a surface is different from the bulk distribution. The surface excess for every chain length can be calculated as

$$\theta^{\rm ex}(N)=M[\phi(N)-\phi^b(N)], \tag{14}$$

where $\phi^b(N)$ is the bulk volume fraction of chains of N segments. Obviously, $\Sigma_N\theta^{\rm ex}(N)=\theta_M^{\rm ex}$.

C. Partition function and equilibrium configuration

The total potential energy U in the system can be expressed as

$$U(\{n_{\alpha\beta}^d(z)\})=\frac{1}{2}\sum_{\alpha,\beta,d,z} n_{\alpha\beta}^d(z)u_{\alpha\beta}, \tag{15}$$

where the factor $\frac{1}{2}$ corrects for double counting of each contact in the sum. In the present study, the only nonzero contribution is that of the 2-2 contacts.

The number of possible configurations in which a certain distribution of states and contacts can be realized is denoted $\Omega(\{n_A^\sigma(z)\},\{n_{\alpha\beta}^d(z)\})$. An expression for this quantity was derived in Ref. [24]:

$$\ln\Omega(\{n_A^\sigma(z)\},\{n_{\alpha\beta}^d(z)\})=-\sum_{A,\sigma,z} n_A^\sigma(z)\ln\phi_A^\sigma(z) - \frac{1}{2}\sum_{\alpha,\beta,d,z} n_{\alpha\beta}^d(z)\ln\frac{\psi_{\alpha\beta}^d(z)}{\phi_\alpha^d(z)}. \tag{16}$$

The first term on the right hand side of this equation corresponds to ideal mixing of monomers. The last term accounts for correlations between the occupations of neighboring sites. The factor $\frac{1}{2}$ accounts for double counting of each contact in the sum. In case of random formation of contacts, $\psi_{\alpha\beta}^d(z)=\phi_\alpha^d(z)$ and the last term in Eq. (16) vanishes.

In order to find the equilibrium state, we have to find the most probable distribution of monomer states and contacts. For a system in open contact with a homogeneous bulk, the equilibrium state can be found by maximization of the grand canonical partition function with respect to the distributions of molecule states $\{n_A^\sigma(z)\}$ and contacts $\{n_{\alpha\beta}^d(z)\}$. The grand canonical partition function is given by

$$\Xi(\{\mu_A\},M,L,T)=\sum_{\{n_A\}} Q(\{n_A\},L,T)\exp\left(\sum_A \frac{n_A\mu_A}{kT}\right) \tag{17}$$

where the sum extends over all distributions $\{n_A\}$ that satisfy constraint (3), and where μ_A is the chemical potential of component A. The canonical partition function $Q(\{n_A\},L,T)$ is a function of the degeneracy Ω and the potential energy U:

$$Q(\{n_A\},L,T)=\sum_{\{n_A^\sigma(z)\},\{n_{\alpha\beta}^d(z)\}}\Omega(\{n_A^\sigma(z)\},\{n_{\alpha\beta}^d(z)\})\times\exp\left(-\frac{U(\{n_{\alpha\beta}^d(z)\})}{kT}\right), \tag{18}$$

where the sum extends over all distributions $\{n_A^\sigma(z)\}$ and $\{n_{\alpha\beta}^d(z)\}$ that satisfy conditions (3) and (4).

Maximization of the grand canonical partition function with respect to $\{n_A^\sigma(z)\}$ and $\{n_{\alpha\beta}^d(z)\}$ considering constraints (3) and (4) gives the distribution of contacts and of molecule states [24]. The distribution of contacts is given by

$$\phi_{\alpha\beta}^d(z)=\frac{\phi_\alpha^d(z)\,\phi_\beta^{-d}(z+\underline{d})}{G_\alpha^d(z)G_\beta^{-d}(z+\underline{d})}\exp\left(-\frac{u_{\alpha\beta}}{kT}\right), \tag{19}$$

where $G_\alpha^d(z)$ is a face weighting factor that accounts for the saturation of faces of type α at layer z having direction d. It is a consequence of constraint (4). For the equilibrium distribution of molecules over the different states we find [24]

$$\phi_A^\sigma(z)=\Lambda_A G_A^\sigma(z) \tag{20}$$

where $\Lambda_A=\exp(\mu_A/kT)$ is a normalization constant. (It has the same value for the heterogeneous system containing the surface as for the homogeneous bulk system with which the heterogeneous system is in equilibrium.) The monomer weighting factor $G_A^\sigma(z)$ measures the probability of finding a molecule of type A having state σ in layer z. It can be factorized as

$$G_A^\sigma(z)=C\prod_{\alpha,d}G_\alpha^d(z)^{q_{A\alpha}^{\sigma d}}, \tag{21}$$

where $q_{A\alpha}^{\sigma d}$ equals 1 if the face pointing in direction d of a molecule A having state σ is of type α, and zero otherwise. Each face of molecule A contributes a factor $G_\alpha^d(z)$ to $G_A^\sigma(z)$. The factor C is a consequence of constraint (3). It can be shown that $C=1$ in homogeneous systems [24]. From this condition the value of C in any system can be found, since Λ_A is identical for systems that are in equilibrium.

The distribution of molecules is normalized by the factor Λ_A. Summation over all states σ and layers z in Eq. (20) yields the following expression for Λ_A:

$$\Lambda_A=\frac{\theta_A}{\sum_{\sigma,z}G_A^\sigma(z)}, \tag{22}$$

where θ_A is the amount of molecules of type A expressed in equivalent lattice layers, $\theta_A=\Sigma_z\phi_A(z)$. Equation (22) makes it possible to normalize any component A by either fixing Λ_A (an open system) or θ_A (a closed system). If the normalization conditions are given for all components, then all face weighting factors $G_\alpha^d(z)$ and volume fractions $\phi_A^\sigma(z)$ are determined completely by Eqs. (19) and (20) and the constraints (3) and (4). These self-consistent equations can be solved numerically as described in Ref. [24], so that the distribution of molecule states and contacts can be found.

D. Limitations of the model

The Bethe-Guggenheim approach adopted in this study takes into account correlations between the occupations of neighboring lattice sites, but the occurrence of contacts is assumed not to depend on other contacts. Although this is not exact, it is much better than the random-mixing approximations of Bragg-Williams and Flory. Taking into account correlations results in an extra term in the expression for packing entropy, Eq. (16). For chain molecules this correction implies a better description of the excluded volume interactions. Whereas in the Flory approximation the excluded volume of a chain of length N is just N times that of a monomer, the present approach implicitly accounts for connectivity. The level at which excluded volume interactions are taken into account is equivalent to Guggenheim's approach [28,29]. For athermal chains with a fixed length this is equivalent to Huggins' treatment [30,31]. This approximation is superior to the Flory approximation. As borne out by simulations by Dickman and Hall [32] it does a far better job in describing the equation of state. The results of the Bethe-Guggenheim approach (and other mean-field theories) for polymer solutions are nearly correct for Θ conditions at all concentrations, and for concentrated solutions at all solvency conditions.

Furthermore, for the present system of bifunctional associating monomers the influence of the possible occurrence of polymeric rings of monomers on the contact probabilities $\psi_{\alpha\beta}^d$ is not accounted for in the Bethe-Guggenheim approximation. It is not so obvious how serious this approximation is. We expect that it is correct for Θ conditions and for concentrated solutions.

In Sec. II B, where the chain length distributions are calculated from the bond probabilities ψ_{22}^d, rings are neglected altogether. It is known [33–35] that rings may contribute significantly at low concentrations for monomers that are of a similar size to the Kuhn length. If the associating monomer is significantly larger or smaller than the Kuhn length, ring closure becomes rare for statistical reasons. For these cases ring closure can be neglected. For monomers that are of similar size to the Kuhn length, the chain length distribution may be different from the one calculated by our model, due to the formation of rings. Still we expect that this will not considerably influence the trends in the concentration profiles and the depletion layer thickness.

III. RESULTS AND DISCUSSION

A. Equilibrium polymers in an isotropic homogeneous system

In an isotropic homogeneous solution, the chain length distribution is exponential, in agreement with mean-field predictions [Eq. (1)]. The average chain length is a function of

the scission energy E and the total volume fraction ϕ_M of monomers. In the well known Flory approximation it is given by Eq. (2). It is interesting to see whether the Bethe-Guggenheim approach yields the same expression.

In an isotropic homogeneous system all site fractions are the same for all layers z and directions d. The site fractions of faces are given by

$$\phi_0^d = 1-\phi_M,$$

$$\phi_1^d = \frac{(q-2)\phi_M}{q}, \tag{23}$$

$$\phi_2^d = \frac{2\phi_M}{q}.$$

The average number of monomers per chain for this case follows from Eqs. (11) and (12) as

$$\langle N\rangle = \frac{\phi_M}{\frac{1}{2}q(\phi_{20}^d+\phi_{21}^d)} = \frac{\phi_2^d}{(\phi_{20}^d+\phi_{21}^d)} = 1+\frac{\phi_{22}^d}{(\phi_{20}^d+\phi_{21}^d)}, \tag{24}$$

where we have used Eq. (23) and constraint (4): $\phi_2^d = \phi_{20}^d + \phi_{21}^d + \phi_{22}^d$. Here ϕ_{22}^d is the site fraction of bonds between monomers in direction d, and $\phi_{20}^d + \phi_{21}^d$ is the site fraction of end segments of the equilibrium polymer chains in direction d [so that $\frac{1}{2}q(\phi_{20}^d+\phi_{21}^d)$ is the number of chains per unit volume].

The distribution of the various contacts between faces is given by Eq. (19), with constraint (4). For $E \gg 0$ we may assume that the number of unfavorable 2-0 and 2-1 contacts is very small. Hence, constraint (4) gives $\phi_0^d \approx \phi_{00}^d + \phi_{01}^d$, $\phi_1^d \approx \phi_{10}^d + \phi_{11}^d$, and $\phi_2^d \approx \phi_{22}^d$. After substitution of Eq. (19) applied to the various contact types we find

$$\phi_0^d \approx \frac{(\phi_0^d)^2}{(G_0^d)^2} + \frac{\phi_0^d\phi_1^d}{G_0^d G_1^d},$$

$$\phi_1^d \approx \frac{\phi_1^d\phi_0^d}{G_1^d G_0^d} + \frac{(\phi_1^d)^2}{(G_1^d)^2}, \tag{25}$$

$$\phi_2^d \approx \frac{(\phi_2^d)^2}{(G_2^d)^2}\exp\left(\frac{E}{kT}\right),$$

where we have used $\phi_\alpha^d = \phi_\alpha^{-d}$ and $G_\alpha^d = G_\alpha^{-d}$. The solution of these equations is $G_0^d = G_1^d = (\phi_0^d + \phi_1^d)^{1/2}$ and $G_2^d = (\phi_2^d)^{1/2}\exp(E/2kT)$. Substitution of these results in Eq. (19) gives the distribution of all contacts. Substitution in Eq. (24) finally yields, with Eq. (23), a relation between the average chain length, the volume fraction of monomers ϕ_M, and the scission energy E:

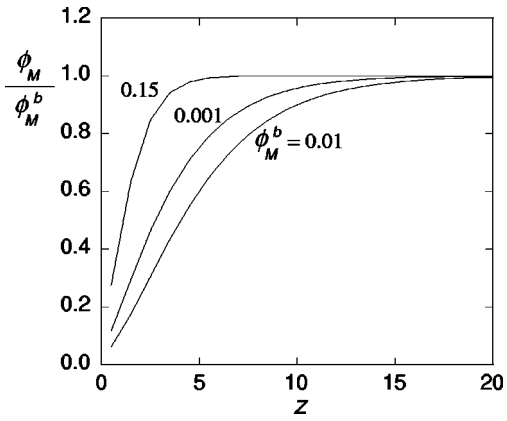

FIG. 2. Monomer volume fraction versus the distance to the surface expressed in lattice layers for three bulk monomer concentrations. The volume fractions have been divided by the bulk volume fraction ϕ_M^b. The scission energy is $15kT$.

$$\langle N\rangle = 1+\left(\frac{\phi_M}{\frac{1}{2}q-\phi_M}\right)^{1/2}\exp\left(\frac{E}{2kT}\right). \tag{26}$$

For $\langle N\rangle \gg 1$ and $\phi_M \ll \frac{1}{2}q$ the Flory result $\langle N\rangle \sim \phi_M^{1/2}$ is found. For larger ϕ_M, however, a correction to this scaling is found: the average length increases more strongly with increasing concentration than the mean-field power law. This correction originates from the connectivity dependence of the excluded volume interactions (see the discussion at the end of Sec. II C). The dependence of the average chain length on the scission energy is the same as in Flory's expression.

B. Depletion at a single surface

The volume fraction of monomers as a function of the distance to a nonadsorbing surface is plotted in Fig. 2 at several bulk concentrations for monomers with a scission energy of $15kT$. The monomer volume fractions have been divided by the bulk volume fraction ϕ_M^b in order to show more detail. At large distance from the surface, the volume fraction of monomers equals ϕ_M^b. Near the surface the volume fraction is lower, because of conformational restrictions, just as for ordinary polymers [1,15,16]. Note that the thickness of the depletion layer is not a monotonic function of the monomer concentration. This will be discussed shortly.

The profiles in Fig. 2 are characterized by the thickness of the depletion layer. Various definitions of the depletion layer thickness Δ may be used [3]. For example, we may replace the continuous profiles by a step function with the same value of $\theta_M^{\rm ex}$. The width of the step function then gives a measure for the depletion layer thickness:

$$\Delta_1 = -\frac{\theta_M^{\rm ex}}{\phi_M^b}. \tag{27}$$

An alternative approach for finding the depletion layer thickness is based on the shape of the volume fraction profile. In

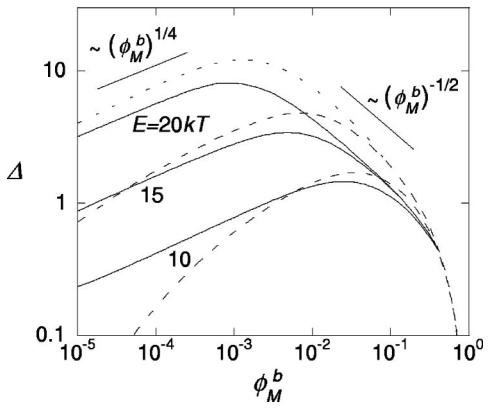

FIG. 3. The depletion layer thickness as a function of the bulk concentration of monomers for three different scission energies. The dashed curves correspond to Δ_1, the full curves to Δ_2.

the asymptotic regime (at large z), the volume fraction approaches the bulk value exponentially:

$$\lim_{z\to\infty}[\phi_M^b-\phi_M(z)]\sim e^{-z/\Delta_2}. \tag{28}$$

The decay length Δ_2 gives an alternative definition of the depletion layer thickness.

Both values of the depletion layer thickness (Δ_1 and Δ_2) are plotted in Fig. 3 as a function of the bulk volume fraction of monomers for various values of E. The two definitions of Δ yield more or less the same trends. At low concentrations, the depletion layer thickness increases with increasing concentration and increasing scission energy. This concentration dependence is different from the behavior observed for ordinary polymers, for which Δ is independent of the concentration in the dilute regime. The reason for this difference is obvious. In dilute solutions, the depletion layer thickness is determined by the (average) radius of gyration of the polymer molecules [3]. For ordinary polymers, the size of the molecules (and thus the radius of gyration) is fixed, but for equilibrium polymers this size increases with increasing concentration [Eq. (2) or (26)]. Therefore the depletion layer thickness also increases. Hence, we expect the following scaling for the depletion layer thickness in the dilute regime:

$$\Delta_d\sim\langle R_g\rangle\sim\langle N\rangle^{1/2}\sim(\phi_M^b)^{1/4}\exp\left(\frac{E}{4kT}\right). \tag{29}$$

Here the second proportionality holds for ideal dilute solutions in a mean-field approximation. For Δ_2 this scaling is found for all values of the scission energy. For Δ_1 this scaling is only found for large values of E, and thus for long chains. At the moment, we do not have an explanation for this.

Once the chains start to overlap, the depletion layer thickness starts to decrease with increasing concentration and it becomes independent of the scission energy (and thus independent of the length of the individual chains). The depletion layer thickness is now determined by the bulk correlation length. In a mean-field approximation, we expect the following scaling for the depletion layer thickness in this regime:

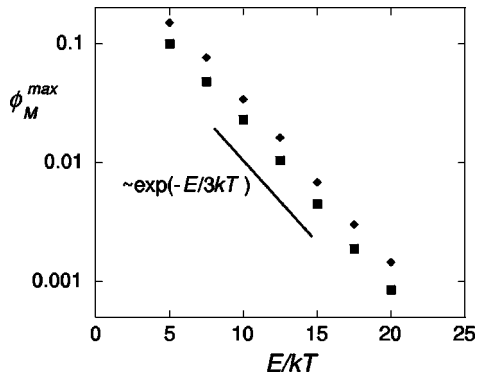

FIG. 4. The volume fraction at which Δ has a maximum as a function of the scission energy E. The diamonds denote the maximum in Δ_1, the squares in Δ_2.

$$\Delta_m\sim\xi_m\sim(\phi_M^b)^{-1/2}, \tag{30}$$

where ξ_m is the correlation length in the marginal regime (see the Introduction). Because the chain length is irrelevant above the overlap concentration, the polydispersity is also unimportant, and the correlation length is the same as for a monodisperse polymer solution. For Δ_2, the marginal regime scaling is clearly visible in Fig. 3, especially at high scission energies. For Δ_1 the marginal regime is more difficult to see. It might be more pronounced at higher E values (longer chains). At high volume fractions the depletion layer thickness decreases more steeply than predicted by Eq. (30). This is due to a crossover to the concentrated regime where higher order interactions become important. Obviously, if the volume fraction goes to unity, the depletion layer thickness goes to zero.

At intermediate concentration the depletion layer thickness exhibits a maximum. The position of the maximum corresponds to the crossover concentration ϕ_M^* from the dilute to the marginal regime. This concentration can be found by equating Δ_d [Eq. (29)] and Δ_m [Eq. (30)]. This yields

$$\phi_M^*\sim\exp\left(-\frac{E}{3kT}\right) \tag{31}$$

and $\phi_M^*\sim\langle N^*\rangle^{-1}$, with $\langle N^*\rangle$ the average chain length at the crossover concentration. The relation between ϕ_M^* and $\langle N^*\rangle$ is the same as for homopolymers (see the Introduction). The position of the maximum is plotted as a function of the scission energy E in Fig. 4, for both definitions of the depletion layer thickness. It can be seen that the position of the maximum is well described by Eq. (31) for both cases.

We may compare our results to the results of Schmitt *et al.* [21]. They considered ideal solutions of equilibrium polymers and derived an analytical expression for the average volume fraction of monomers in a gap between repulsive walls. In the limit of infinite gap width their results give for the surface excess at a single surface $\theta_M^{ex}/\phi_M^b\sim\langle R_g\rangle$, which is in agreement with our results for the dilute regime [Eq. (29)].

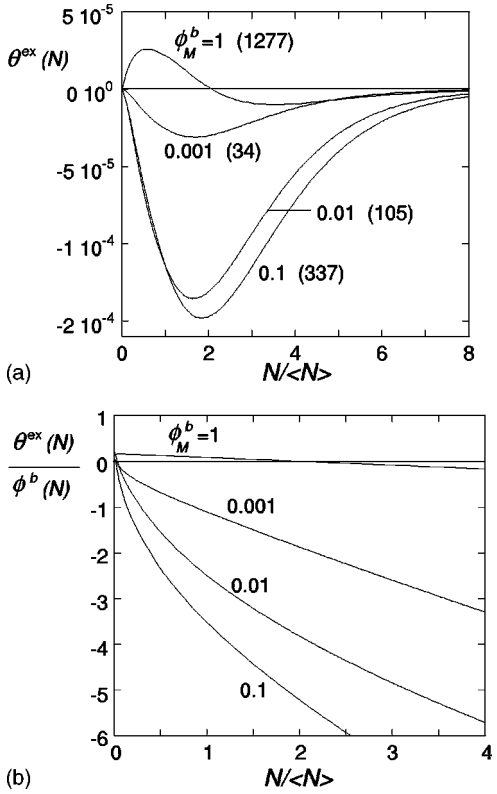

FIG. 5. (a) The excess amount $\theta^{\mathrm{ex}}(N)$ as a function of chain length for several values of ϕ_M^b and $E=15kT$. Average lengths are indicated in parentheses. (b) $\theta^{\mathrm{ex}}(N)/\phi^b(N)$ versus the chain length for the same parameters.

C. Chain length distribution at a surface

The total excess amount of monomers near the surface θ_M^{ex} is the sum of the contributions $\theta^{\mathrm{ex}}(N)$ of all chain lengths in the solution. The excess amount of each component as a function of its chain length is plotted in Fig. 5(a) for several monomer concentrations ϕ_M^b and a scission energy of $15kT$. The chain length has been divided by the average chain length in order to show more detail. Fig. 5(b) shows $\theta^{\mathrm{ex}}(N)/\phi^b(N)$ as a function of the chain length for the same data. It is obvious that the distribution of chain lengths near the surface differs from the bulk composition. The effect of the surface is different for chains of different length. From Fig. 5(b) it can be seen that the region close to the surface is preferably occupied by the shorter chains, in agreement with previous findings [18,19]. This is because the conformational restrictions near the surface are smaller for short chains than for long ones. The relation between $\theta^{\mathrm{ex}}(N)$ and N is different below and above the overlap concentration. In the dilute regime, all $\theta^{\mathrm{ex}}(N)$ are negative, i.e., all chains are depleted from the surface. There are no interactions between chains in this regime, so that the concentration profile of every component in the solution is the same as for a monodisperse solution of chains of the same chain length and bulk concentration. Hence, every component has a depletion layer with a characteristic depletion layer thickness $\Delta(N)$, which is not influenced by the other components in solution. Again $\Delta(N)$ may be defined in different ways, but here we only use $\Delta_1(N)$ [Eq. (27)]. For long enough chains $\Delta_1(N)$ is proportional to the radius of gyration $R_g(N)\sim\sqrt{N}$ of chains of length N. Hence, in the dilute regime we find

$$\frac{\theta^{\mathrm{ex}}(N)}{\phi^b(N)}=-\Delta_1(N)\sim-\sqrt{N}. \tag{32}$$

Because $\phi^b(N)$ has a maximum at $N=\langle N\rangle$, the excess amount $\theta^{\mathrm{ex}}(N)$ [Fig. 5(a)] has a minimum. It is easily shown that substitution of Eq. (1) in Eq. (32) yields a minimum in $\theta^{\mathrm{ex}}(N)$ at $N=\frac{3}{2}\langle N\rangle$, which is also seen in Fig. 5(a).

In more concentrated solutions relation (32) no longer holds. The chains overlap and interactions between the chains become dominant. This is most clearly seen in the melt, where the total volume fraction of monomers is unity, and hence the total surface excess of monomers θ_M^{ex} is zero. The larger entropic penalty near the surface causes a depletion of long chains. This depletion must be compensated by a net adsorption of short chains. The surface segregation in polydisperse polymer melts has been investigated before [18,20]. It was shown that the following relation holds for polydisperse polymer melts, irrespective of the chain length distribution [20]:

$$\frac{\theta^{\mathrm{ex}}(N)}{\phi^b(N)}=A\left(1-\frac{N}{\langle N\rangle_w}\right), \tag{33}$$

where $\langle N\rangle_w$ is the weight averaged chain length, and where $A\approx0.195$ in a cubic lattice. The results in Fig. 5(b) are in agreement with these results. In an exponential chain length distribution, $\langle N\rangle_w=2\langle N\rangle$. Hence, the intercept with the horizontal axis is at $N=2\langle N\rangle$.

With increasing monomer concentration there is a transition from the dilute regime [Eq. (32)] to the concentrated regime [Eq. (33)]. Just like the total depletion layer thickness (Fig. 3), the depletion layer thickness $\Delta(N)$ of every component exhibits a maximum around the overlap concentration.

IV. CONCLUDING REMARKS

In this paper we applied a model for molecules with orientation dependent interactions, based on a Bethe-Guggenheim approximation, to a system of equilibrium polymers. The model can be used in both homogeneous and inhomogeneous systems. The chain length distribution in a homogeneous system is in agreement with Flory's mean-field predictions, with small corrections at high monomer concentrations.

For equilibrium polymers at a nonadsorbing surface we found that the depletion layer thickness has a maximum at the crossover concentration from the dilute to the marginal regime. In the dilute regime the depletion layer thickness is proportional to the average radius of gyration, and in the marginal regime it corresponds to the bulk correlation length ξ_m. In this paper, intra- and intermolecular segment-segment interactions are accounted for on a mean-field level. Such a mean-field treatment does not account for the swelling of the polymer coils in a good solvent. The excluded volume inter-

actions result in an expansion of the chains [1,2]: the radius of gyration R_g in a good solvent is proportional to $N^{3/5}$ rather than $N^{1/2}$. Hence, the exponents in Eq. (29) are not correct for a good solvent. Furthermore, the mean-field approach is not able to describe the semidilute regime, where the correlation length scales as [1,19] $\xi_s \sim \phi^{-3/4}$. We expect that the thickness of the depletion layer still has a maximum for swollen chains in a good solvent. The position of this maximum may depend in a different way on E and T than predicted by Eq. (31), however. For many practical systems the crossover from the semidilute to the marginal regime occurs at relatively low volume fractions [3]. In the marginal regime, the mean-field approach is justified. Also, in most cases the solvent is not athermal, so that excluded volume interactions are screened to some extent. In Θ solvents the mean-field treatment is effectively exact. Therefore, we expect that our model becomes more accurate if we introduce a net attraction between polymer segments ($u_{11}, u_{12} < 0$). This extension is straightforward.

The experimental evidence for depletion of equilibrium polymers is scarce. Kékicheff *et al.* [36] measured the depletion interaction between two mica surfaces in a solution of wormlike micelles of CTAB above the overlap concentration. The range of the depletion attraction was found to decrease with increasing surfactant concentration, in agreement with our results for concentrations above the overlap concentration. The exponent α for the correlation length $\xi \sim \phi^{-\alpha}$ was approximately 0.65, which falls between marginal and semidilute scaling. No measurements for dilute solutions of equilibrium polymers are reported yet, and hence also the maximum in the depletion layer thickness has not been found yet experimentally.

In Sec. III C we studied the surface segregation of chains of different lengths. Small chains reside preferably in the surface region. In the dilute regime every component in the mixture is depleted from the surface to a distance comparable to its radius of gyration. With increasing concentration, a net adsorption is observed of short chains. In the melt, there is a linear relation between $\theta^{\mathrm{ex}}(N)/\phi^b(N)$ and N, and $\theta^{\mathrm{ex}}(N)$ changes sign at $N = \langle N \rangle_w$.

The model described in this paper is very versatile. It can be used to calculate the effect of an equilibrium polymer solution on the interactions between two surfaces, for both adsorbing and nonadsorbing polymers. Furthermore, semiflexible or rodlike equilibrium polymers can be modeled by assigning a positive energy to bent monomer states. We can also study associating molecules that occupy more than one lattice site. In this way we can model associating monomers that are larger or smaller than the Kuhn length. We expect, however, that the trends for these cases will be the same as predicted in this paper. Other interesting possibilities include the study of end-grafted equilibrium polymers (''equilibrium brushes''), branched equilibrium polymers, and the effect of ''chain stoppers'' (monomers with only one bonding group). These aspects will be the subject of future publications.

ACKNOWLEDGMENT

The research of N. A. M. Besseling was made possible by support from the Royal Dutch Academy of Arts and Sciences.

[1] P. G. De Gennes, *Scaling Concepts in Polymer Physics* (Cornell University Press, Ithaca, NY, 1979).
[2] P. J. Flory, *Principles of Polymer Chemistry* (Cornell University Press, Ithaca, NY, 1953).
[3] G. J. Fleer, M. A. Cohen Stuart, J. M. H. M. Scheutjens, T. Cosgrove, and B. Vincent, *Polymers at Interfaces* (Chapman and Hall, London, 1993).
[4] R. L. Scott, J. Phys. Chem. **69**, 261 (1965).
[5] J. C. Wheeler, S. J. Kennedy, and P. Pfeuty, Phys. Rev. Lett. **45**, 1748 (1980).
[6] S. J. Kennedy and J. C. Wheeler, J. Phys. Chem. **78**, 953 (1984).
[7] M. E. Cates and S. J. Candau, J. Phys.: Condens. Matter **2**, 6869 (1990).
[8] R. P. Sijbesma, F. H. Beijer, L. Brunsveld, B. J. B. Folmer, J. H. K. K. Hirschberg, R.F.M. Lange, J.K.L. Lowe, and E.W. Meijer, Science **278**, 1601 (1997).
[9] P. J. Flory, J. Am. Chem. Soc. **58**, 1877 (1936).
[10] T. F. Tadros, in *The Effect of Polymers on Dispersion Properties*, edited by T. F. Tadros (Academic Press, New York, 1982), p. 1.
[11] B. Yarar, in *Solution Behavior of Surfactants*, edited by K. L. Mittal and E. J. Fendler (Plenum, New York, 1982), p. 1333.
[12] D. H. Napper, *Polymeric Stabilization of Colloidal Dispersions* (Academic Press, London, 1983).
[13] J. M. H. M. Scheutjens and G. J. Fleer, J. Phys. Chem. **83**, 1619 (1979).
[14] J. M. H. M. Scheutjens and G. J. Fleer, J. Phys. Chem. **84**, 178 (1980).
[15] J. M. H. M. Scheutjens and G. J. Fleer, Adv. Colloid Interface Sci. **16**, 361 (1982).
[16] G. J. Fleer and J. M. H. M. Scheutjens, Croat. Chem. Acta **60**, 477 (1987).
[17] A. Y. Grosberg and A. R. Khokhlov, *Statistical Physics of Macromolecules* (AIP, New York, 1994).
[18] A. Hariharan, S. K. Kumar, and T. P. Russell, Macromolecules **23**, 3584 (1990).
[19] A. Hertanto and R. Dickman, J. Chem. Phys. **93**, 774 (1990).
[20] J. Van der Gucht, N. A. M. Besseling, and G. J. Fleer (unpublished).
[21] V. Schmitt, F. Lequeux, and C.M. Marques, J. Phys. II **3**, 891 (1993).
[22] A. Milchev and D. P. Landau, J. Chem. Phys. **104**, 9161 (1996).
[23] Y. Rouault and A. Milchev, Macromol. Theory Simul. **6**, 1177 (1997).
[24] N. A. M. Besseling and J. M. H. M. Scheutjens, J. Phys. Chem. **98**, 11597 (1994).
[25] N. A. M. Besseling and J. Lyklema, J. Phys. Chem. **98**, 11610 (1994).

[26] N. A. M. Besseling and J. Lyklema, Pure Appl. Chem. **67**, 881 (1995).
[27] N. A. M. Besseling, Langmuir **13**, 2113 (1997).
[28] E. A. Guggenheim, *Mixtures* (Oxford University Press, London, 1952).
[29] E. A. Guggenheim, Proc. R. Soc. London, Ser. A **183**, 203 (1944).
[30] M. L. Huggins, Ann. N.Y. Acad. Sci. **43**, 1 (1944).
[31] M. L. Huggins, J. Chem. Phys. **9**, 440 (1941).
[32] R. Dickman and C. K. Hall, J. Chem. Phys. **85**, 3023 (1986).
[33] H. Jacobson and W. H. Stockmayer, J. Chem. Phys. **18**, 1600 (1950).
[34] P. van der Schoot and J. P. Wittmer, Macromol. Theory Simul. **8**, 428 (1999).
[35] J. P. Wittmer, M. Milchev, P. van der Schoot, and J.-L. Barrat, J. Chem. Phys. **113**, 6992 (2000).
[36] P. Kékicheff, F. Nallet, and P. Richetti, J. Phys. II **4**, 735 (1994).